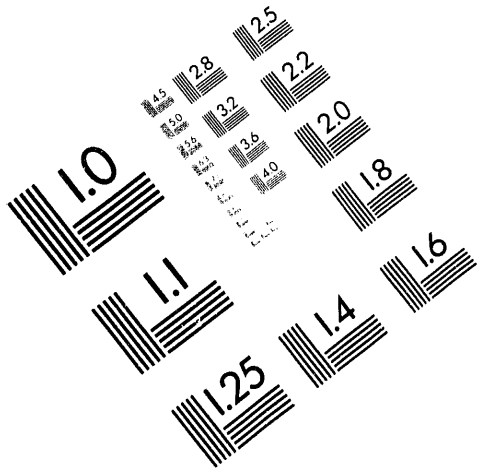



**Association for Information and Image Management**

1100 Wayne Avenue, Suite 1100
Silver Spring, Maryland 20910

301/587-8202

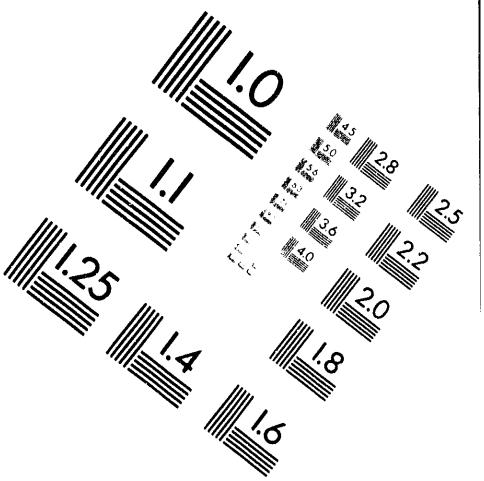


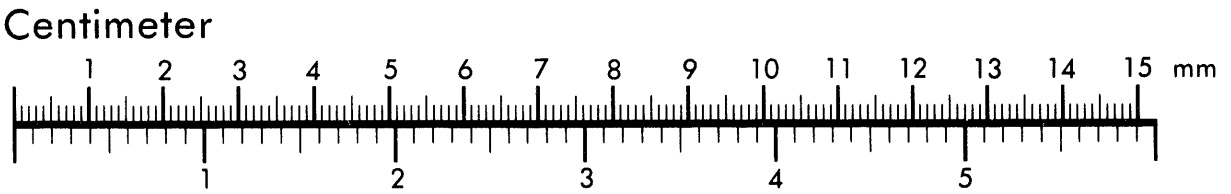


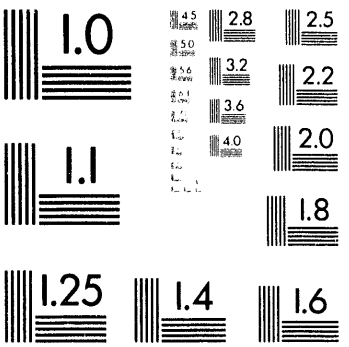


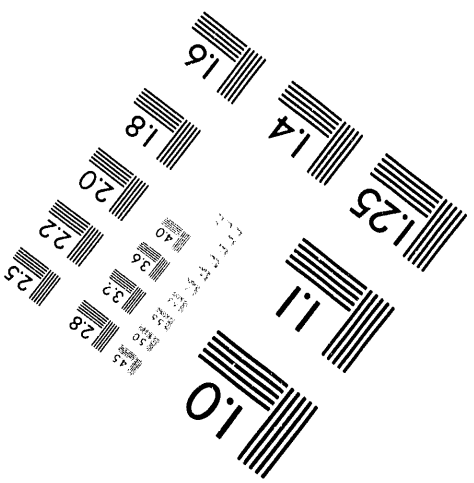


MANUFACTURED TO AIIM STANDARDS
BY APPLIED IMAGE, INC.

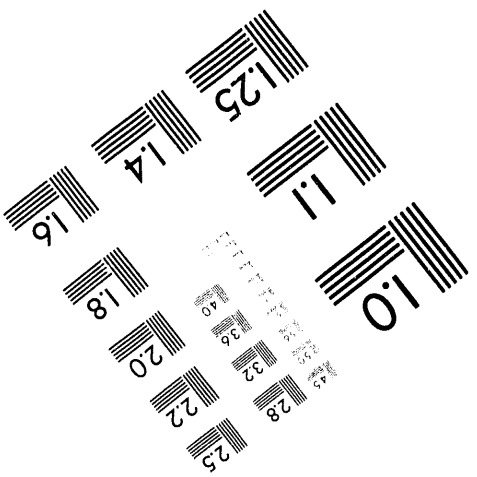

1 of 1

DRAFT COPY - TO BE PRESENTED AT THE 44TH ECTC MAY 1994

# EVALUATING PLASTIC ASSEMBLY PROCESSES FOR HIGH RELIABILITY APPLICATIONS USING HAST AND ASSEMBLY TEST CHIPS*



John A. Emerson, James N. Sweet, David W. Peterson,
Sandia National Laboratories
P. O. Box 5800
Albuquerque, NM 87185-0958

*Abstract*—**We demonstrate the use of HAST and Assembly Test Chips to evaluate the susceptability of epoxy molding compounds to moisture induced corrosion of Al conductors. We show that the procedure is sufficiently sensitive to discriminate between assembly processes used by different molding facilities. Our data show that the location in time of the "knee" in the failure distribution is dependent on material properties of the epoxy. Reducing the failure rate in the early or "extrinsic" region of the time-failure distribution is key to achieving high reliability. We examine the failure modes in the extrinsic region for test chips encapsulated with a number of high quality molding compounds in an attempt to better understand this region.**

## INTRODUCTION

This paper represents a continuation of our work involving the evaluation of the protective properties of organic encapsulants for microelectronic packaging [1 ]. In ref. 1, we described the Highly Accelerated Stress Test (HAST) performance of liquid organic encapsulants intended for chip-on-board (COB) or cavity-fill applications. Moisture induced corrosion failures in organically packaged systems depend on both the properties of the organic encapsulant or molding compound and factors associated with the assembly process. In this paper, we describe the HAST performance of some epoxy molding compounds chosen for their ability to retard moisture activated corrosion. In addition, two different assembly facilities were used in an attempt to discriminate between assembly processes. The intent of this work was not to define a "best" materials or vendors list for high reliability molding operations, but to contribute toward a comprehensive procedure for defining such a list. The four molding compounds used in this experiment were obtained from venders as characteristic of their best product at the time for preventing moisture activated corrosion. We have elected not to explicitly identify the manufacturers of these materials because our experiments did not involve statistically significant sample sets.

## BACKGROUND

From previous HAST on plastic encapsulated ICs, it has been shown that the failure fraction vs. time function (failure rate curve) has three distinct regions [1],[2 ],[3 ]. A failure distribution function is characterized by the time to 50% failure, $t_{50}$, and a standard deviation. In general these failure distributions are well described by a composite log-normal function. Fig. 1 shows representative failure data for plastic encapsulated Sandia Assembly Test Chips (ATCs) collected during HAST experiments at 140 °C, 85% relative humidity (RH) and 40 VDC track bias. The design and use of these test chips are described elsewhere [4 ]. The curves show data from this work which describes the failure rate of liquid epoxy glob top parts, transfer molded parts and silicone gel coated parts. Three characteristic regions are apparent in the epoxy curves. The first region, which occurs at the earliest test times, is described by a distribution function with a small slope (long projected $t_{50}$). This part of the failure distribution, often called the "extrinsic" region, is associated with random failures produced by defects introduced in the manufacturing process. The third region occurs at the longest times and is recognized by an observable increase in the slope of the failure distribution. This region is sometimes called the "intrinsic" or wear-out region. Failures in this region are in some way tied to processes or reactions associated with the material and the environment. Between these two regions is a "knee" marking the transition between the two failure distributions and, presumably, two primary failure modes.

Referring to Fig. 1, the epoxy glob top curve clearly shows the three regions with the knee of the curve at about 150 h. The data for the epoxy molding compound shows a similar extrinsic failure rate, but the knee is extended further in time ≈ 1000 h. In the case of the silicone gel, the knee has not been reached during the accessible test times, but may be starting at 2000 h. The position of the knee is primarily dependent on intrinsic failure modes and can be moved further in time by selection of increasingly superior materials and processes. This is illustrated in Fig. 1 by the replacement of liquid epoxy with a molded epoxy encapsulant.

High reliability in plastic parts is primarily associated with reducing the failure rate in the extrinsic region. Failure rates in the extrinsic region are related to defects in the die, the molding compounds and the assembly process. In the present work, special attention is devoted to examining the extrinsic failure region.

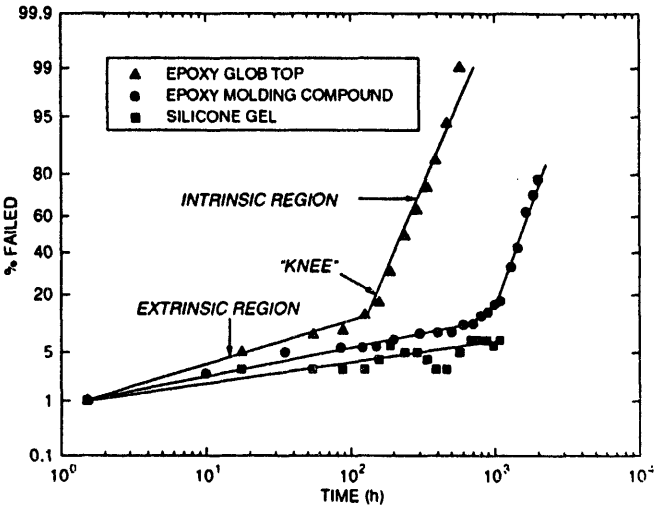


Fig. 1. Typical experimental data from HAST of ATC01 corrosion test chips coated with silicone and epoxy liquid encapsulants. Tests were performed at 140°C, 85% RH and 40 VDC track bias, and data is for anodic tracks only. The curves show characteristic intrinsic and extrinsic failure regions. Straight lines have been drawn to aid the reader in observing the distribution of the data, not to represent a data fit.



* This work performed at Sandia National Laboratories is supported by the U.S. Department of Energy under contract DE-AC04-94AL85000.

## Experimental Setup

From our previous work on HAST of liquid encapsulants, we saw how different material classes affect the failure distribution [1]. For this work, a narrower material class, epoxy molding compounds, was chosen to examine the effect of assembly process variations and what we believe to be small material differences. Four different molding compounds were chosen with similar published material properties. The vendors's recommended processing parameters were used for application and curing.

TABLE I.
CLEANING PROCEDURE USED BY EMANUEL

| Operation | Time | Temperature |
|---|---|---|
| Freon® | 5 min | Vapor |
| Freon® | 5 min | Room temperature |
| 18 MΩ $H_2O$ (D.I.) | 15 min | Room temperature |
| Bake (Class 100) | 1 hour | 120°C |

Two independent molding contractors were used to assemble and transfer mold the ATC01 test chips used in this work. One contractor, the "blind," received no input from the authors on cleaning, lead frame material, and processing conditions; only the lot number of molding compound was known. The other contractor, Emanuel Equipment, assembled parts under carefully controlled conditions using cleaning and handling procedures specific to this experiment. Lead frames were alloy-42 (42% Ni; 58% Fe) Au plated on the paddle area, wire bond pads, and exposed external contacts. To ensure maximum adhesion, all areas of contact between the molding compound and the lead frame were to Alloy-42 except the Au areas near the chip. Class 100 clean room conditions were maintained throughout the assembly operation from die bonding through molding. Standard die attach (Ablestik 84-1LM1 cured at 150°C - 1h) and Au wire (1.25 mil) bonding procedures were followed. Prior to molding, the parts were cleaned as shown in Table I.

TABLE II.
MOLDING COMPOUNDS AND PROCESSING PARAMETERS

| Group | Molder | Mold Temp. (°C) | Cycle Time (sec) | Post Cure |
|---|---|---|---|---|
| MC1 | Emanuel | 185 | 120 | 175° - 6 h |
| MC2 | Emanuel | 185 | 120 | 175° - 5 h |
| MC3A | "Blind" | | | |
| MC3B | Emanuel | 185 | 120 | 175° - 8 h |
| MC4A | "Blind" | | | |
| MC4B | Emanuel | 185 | 120 | 175° - 8 h |

The time interval between final clean and molding was kept under 1 h. Table II contains the specific materials and curing parameters used for each molding compound. Because the overall aim of this work is toward plastic package testing methodology rather than product evaluation, we chose not to identify the molding compounds listed in Table II.

TABLE III.
TRIPLE TRACK PARAMETERS

| TT No. | $w_{Al}$ (μm) | $w_g$ (μm) | ε field (MV/m) @ 40 VDC |
|---|---|---|---|
| 2 | 2 | 2 | 20 |
| 4 | 4 | 4 | 10 |
| 5 | 5 | 6 | 6.7 |
| 6 | 6 | 4 | 10 |

The ATC01 chips used for this experiment were all passivated with 1.2 μm thick 3% P doped $SiO_2$, deposited by low pressure chemical vapor deposition (LPCVD) at 400°C. Four of the seven triple tracks on ATC01 were used: TT2, 4, 5, and 6. The Al linewidths, $w_{Al}$, and line-to-line gaps, $w_g$, of these tracks are shown in Table III.

HAST conditions were 140°C/85% RH, +40 V bias on outer tracks with respect to the center track using the standard triple track configuration. Offline measurements of track resistance were made at room temperature using general purpose data acquisition and control equipment. A failure is defined as an increase in track resistance of 100% over previous measurements. The failure fraction is the number of failed tracks divided by the total number of available tracks. Table IV contains total numbers of tracks for each group and HAST test times at completion. Measurements were repeated on tracks with high readings to ensure they were not false indications. High readings which later returned to acceptable levels were classified as failures at the original observation time. Intermittent high readings are not uncommon during HAST on encapsulated parts and have been attributed to fractures in the bond wire to bond pad interface. The encapsulant keeps the wires in place so that electrical connections make and break during thermal transients.

TABLE IV
TRACK COUNT AND TEST TIMES

| Group | No. Anodic Tracks | No. Cathodic Tracks | Duration of Testing |
|---|---|---|---|
| MC1 | 288 | 144 | 1400 h |
| MC2A | 144 | 72 | 1400 h |
| MC2B | 175 | 100 | 2060 h |
| MC3A | 357 | 204 | 1400 h |
| MC3B | 386 | 220 | 1400 h |
| MC4A | 372 | 212 | 1400 h |
| MC4B | 424 | 212 | 2000 h |

Prior to HAST testing, all parts except group MC4B were temperature cycled between -65° and 150° for 100 cycles according to MIL-STD-883C Method 1010 Condition C. Following temperature cycling and immediately after an aqueous cleaning operation, the parts from each experimental group except MC4B were distributed across eight HAST boards. HAST on the MC4B group was conducted at an earlier time in conjunction with an unrelated experiment. In both cases, part location was randomized and preserved during all subsequent testing. The parts were periodically removed from the HAST chamber for offline electrical testing and returned to the chamber for further HAST. At the first offline testing interval (10 h), a single failed part from each experimental group (except MC4B) was removed for failure analysis. Although not statistically significant, these early failures provided an opportunity to examine the failure mechanism at work in the extrinsic region of each experimental group. At the completion of testing, encapsulant was removed with hot flowing $H_2SO_4$ to expose the bond wires and die surface. Failure analysis was done by standard optical, SEM, and EDAX methods.

## Experimental Results

No electrical failures were observed after temperature cycling. The failure distributions for anodic tracks in the MC1 and MC2 groups assembled at Emanuel are shown in Fig. 2. Cathodic failure data have similar distributions, but with longer failure times. Note that the failure distributions in the extrinsic region are similar, but the knee occurs at ≈ 300 h for MC1 and has not appeared yet by 2000 h for the MC2A group. The MC2B group was not part of this experiment, but the assembly was done at the same time and place as the MC2A group using the same molding compound lot. In addition to thermal cycling, the MC2B group was subjected to salt spray. HAST was done in the same chamber, but at a different time. The MC2B group has a higher

failure rate in the extrinsic region than the MC2A group, but seems to be converging on the same knee.

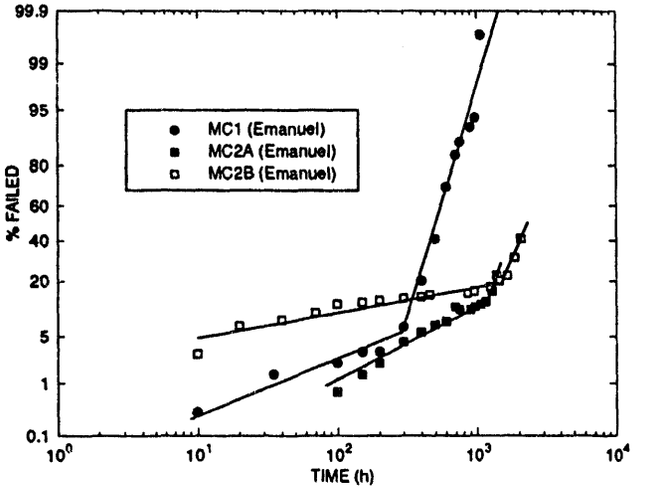


Fig. 2. Failure distribution of ATC01 triple tracks during HAST at 140 °C, 85% RH and 40 VDC. Data is shown for MC1 and MC2 anodic tracks only; cathodic track data is similar.

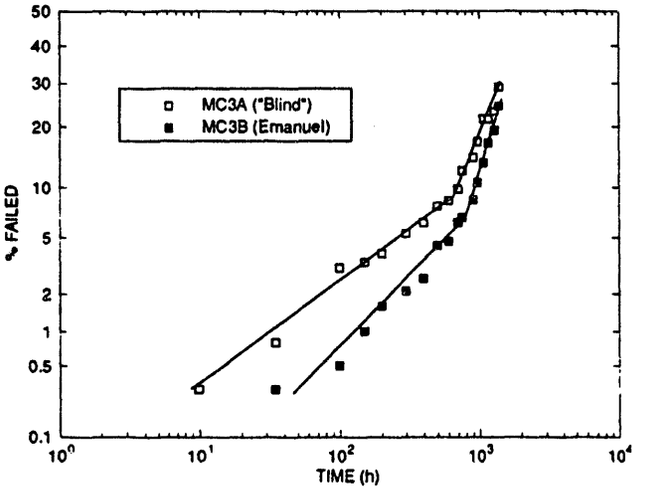


Fig. 3. Plot of MC3 data, "Blind" vs. Emanuel, showing slightly better overall HAST life expectancy of parts assembled at Emanuel.

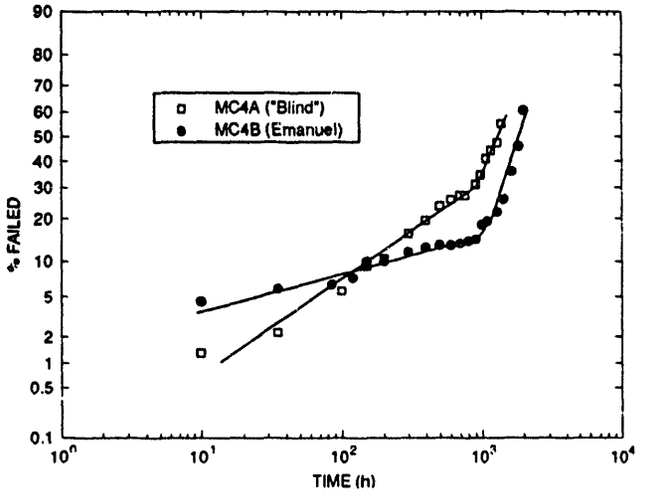


Fig 4. Plot of MC4 data showing similar relation to Fig. 3 in the intrinsic region for parts assembled at "Blind" and Emanuel . The MC4B parts were assembled at the same time as MC4A but were tested to 2000 h during an unrelated experiment.

Figs. 3 and 4 contain failure data for the MC3 and MC4 molding compounds. The open symbols represent the "blind" group and the solid symbols represent the controlled assembly (Emanuel) group. The MC3 data in Fig. 3 show that the controlled assembly process resulted in better HAST performance. The MC4 data in Fig. 4 show a similar relation, although the early failure distribution for the MC4B group appears quite different than the MC4A group. The reason for the disparity in the extrinsic region is not known at this time.

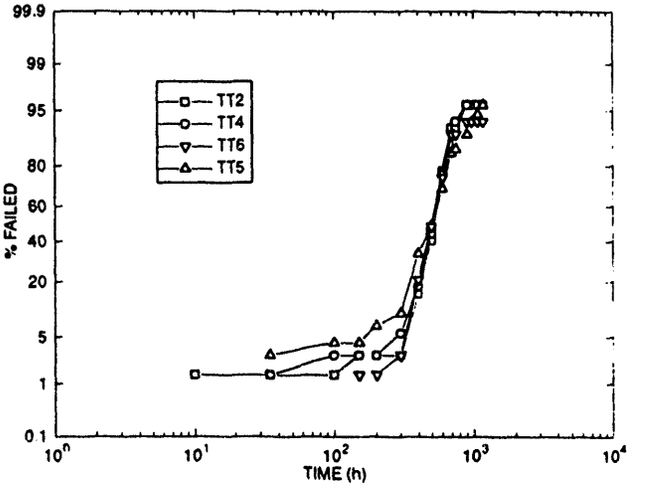


Fig. 5. Plot of MC1 anodic track data by triple track type. Order from top to bottom in legend is toward decreasing ε field. Refer to Table III for track parameters.

The failure rate for the MC1 molding compound is shown as a function of triple track type, *i.e.*, track spacing. If the failure rate depended on the ε field between adjacent tracks, there should be a dependence evident on track type. There is no obvious dependence of the failure rate in Fig. 5 on track type.

TABLE V
FAILURE ANALYSIS OF 10 h PARTS

| Group | Electrical Test | | Optical Inspection | | |
|---|---|---|---|---|---|
| | 10 h | After Decap | Open Track | Open Pad | Unbonded Pad Corrosion |
| MC1 | TT2I | TT2I | x | | yes |
| | | TT2O | x | | |
| | | TT2C | x | | |
| | | TT4C | x | | |
| | | TT5O | | x | |
| | | TT5C | | x | |
| | | TT5I | | x | |
| | | TT6O | | x | |
| MC2 | TT4C | TT4C | | x | no |
| | | TT5O | | x | |
| MC3A | TT5C | TT5C | | x | yes |
| MC3A | TT2C | TT2C | | x | yes |
| MC3B | TT2C | TT2C | | x | yes |
| | | TT5C | | x | |
| MC4A | TT5I | | | | yes |
| | | TT2O | | x | |
| | | TT4O | | x | |
| | | TT5O | | x | |
| | | TT5C | | x | |
| | | TT6O | | x | |
| | | TT6C | | x | |

Each experimental group had one or more parts showing a single open track after the 10 h electrical test. One part was removed from test out of the MC1, MC2, MC3B, and MC4A groups. Two parts were removed from the MC3A group. The results of microscopic examination of these early failures are contained in Table V, where the failed triple track is identified by "O" for outer track, "C" for center track, and "I" for inner track. Although corrosion in the high electric field region of the triple track was apparent in at least one case, the overwhelming observation was of corrosion on both bonded and unbonded (and unbiased) pads. The appearance of the unbonded pads ranged from mild discoloration to complete abscence of Al metalization down to interlevel dielectric. The bond pads shown in Fig. 6 are typical. Additional electrical failures were observed in 4 of the 6 parts after encapsulation was removed. In the case of the MC1 and MC4A parts, these additional failures were substantial. It is not clear whether this is indicative of a continuing corrosion process after HAST or whether the molding compound was preserving an electrical path by physical constraint.

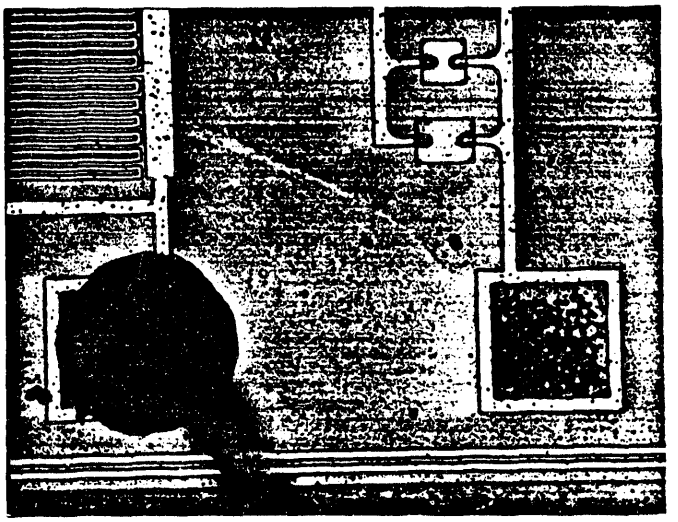

Fig. 6. Photomicrograph of MC4A part which failed after 10 h of HAST showing complete removal of Al on a Au ball-bonded pad. The bonded pad is to an unbiased test structure not used during this experiment. Corrosion and Al depletion is also evident on an adjacent unbonded pad.

Further failure analysis of the bond pad, triple track, and the overall surface of the ATC samples by EDAX did not reveal any impurities that could lead to corrosion. Our limit of detection was about 0.1 atomic %. EDAX analysis of cleaved molding compound that was taken from the set of removed 10 h samples showed Si, Br, Sb, and Fe. In parts, such as MC1, higher concentrations of Br were observed than in the MC3A&B samples. Br and Sb are standard flame retardant additives.

Beyond the knee, or in the intrinsic failure regime, failures were dominated by bond pad corrosion and bond wire separation. In some cases, corrosion extended underneath the chip passivation out into the triple track region. No dendrite growth or intertrack shorting was observed. Corrosion occurred at both anodic and cathodic biased bond pads and also at bonded but unbiased pads. The failure rate did not depend on track-to-track spacing as discussed above. Figs. 7-9 contain SEM photomicrographs of an MC4B part after 2000 h of HAST at 140 °C, 85% RH and 40 VDC bias. They are representative of virtually all the decapsulated parts at the completion of testing.

## Discussion of Results

*Mold compound discrimination*

Fig. 2 indicates that HAST can discriminate between molding compounds used for high reliability applications. The $t_{50}$ for the MC2 compound is at least a factor of 2 greater than that of the MC1 compound. This is consistent with chemical analysis of the two materials showing that MC1 had a higher Br content [5 ],[6 ]. This difference is significant considering that both compounds are in a family of materials with very little variation in their formulation.

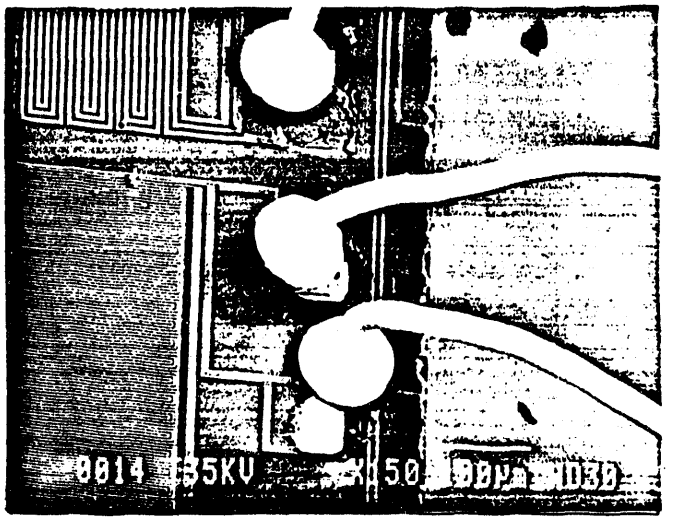

Fig. 7. SEM photomicrograph of MC4B part after 2000 h of HAST. Note depletion of Al in upper anodic bond pad and Au deposit on cathodic bond pad at bottom. Top triple track structure is TT6, bottom is TT2.

Although two distinct slopes are observed in the failure distributions for all of the parts in this experiment, we were unable to determine any difference in failure mechanisms for failures in the two regions. We speculate that extrinsic failures are produced by corrosion enhancement mechanisms such as contamination in the molding compound or poor surface adhesion in localized areas.

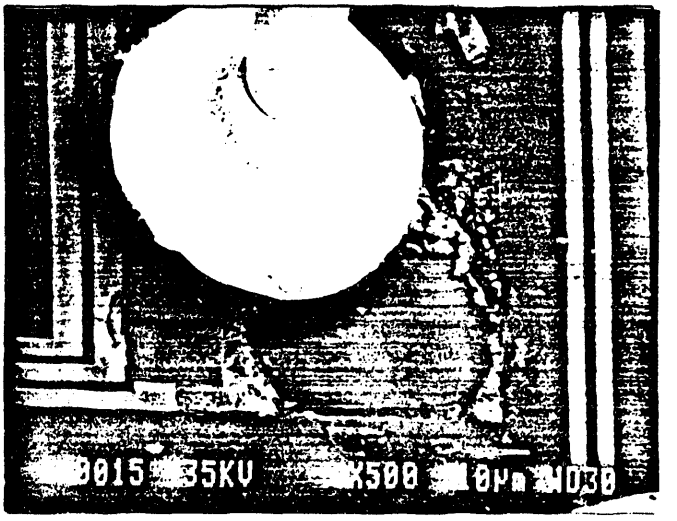

Fig. 8. SEM photomicrograph showing enlarged view of upper bond pad of MC4B part in Fig. 7. The cracked and delaminated P-glass visible adjacent to the bond pad is caused by corrosion of the underlying Al tracks.

*Assembly contractor discrimination*

The data in Figs. 3 and 4 show that carefully controlled assembly performed by Emanuel resulted in slightly better HAST performance than the "blind" vendor. These data are consistent with the hypothesis that only the extrinsic failure distribution varies between the two molding contractors. The intrinsic portions of the failure distributions in Figs. 3 and 4 for the two molding contractors have approximately the same slope and mean value. We did not observe any difference in failure modes between the parts in these two populations. The fact that

the improved HAST lifetime for the Emanuel assembled parts was observed across two different molding compounds adds validity to our assertion that HAST can discriminate between molding contractors.

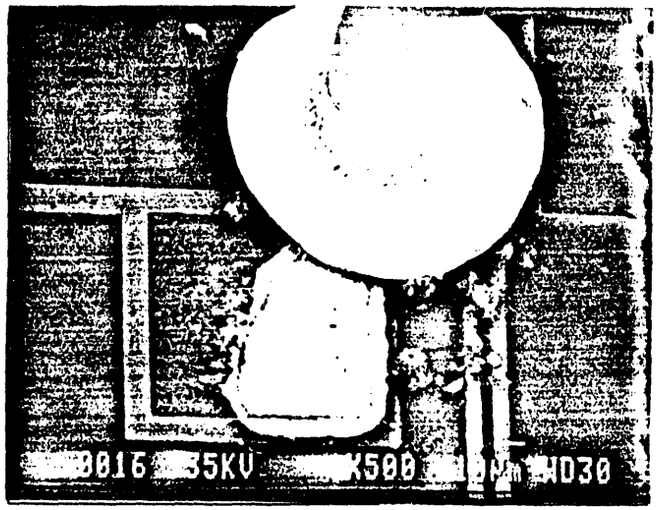


Fig. 9. SEM photomicrograph showing enlarged view of lower bond pad of MC4B part in Fig. 7. Note the presence of Au intermetallics on the Al bond pad.

## CONCLUSIONS

We have demonstrated that the HAST performance of transfer molded ATC01 parts is well described by a composite log-normal distribution. Our data show that nominally identical molding compounds can produce a large observable difference in HAST performance. Our experiment to discriminate between two different molding contractors resulted in small but discernable differences in HAST lifetime in each of two different molding compounds. Further experimentation is required to clarify the nature of failures in the extrinsic region. It is not clear at this time how to decrease the failure rate in the extrinsic region. Such a reduction is necessary if plastic is to be applied to high reliability applications.

## REFERENCES


[1] J. A. Emerson, D. W. Peterson and J. N. Sweet, "HAST Evaluation of Organic Liquid IC Encapsulants using Sandia's Assembly Test Chips," *in Proceedings of 42nd Electronic Components & Technology Conference*, 1992, pp.951-956.

[2] D. Danielson, G. Marcyk, E. Babb, and S. Kudva, "HAST Applications: Aceleration Factors and Results for VLSI Components," *Proc. 27th Annual Reliability Physics Symposium*, IEEE, 1989, pp. 114-121.

[3] J. W. Osenback, "Water-Induced Corrosion of Materials Used for Semiconductor Passivation," J *Electrochem. Soc*, vol 140, pp. 3667-3675, December 1993.

[4] J. N. Sweet, D. W. Peterson, M. R. Tuck, D. J. Renninger, *Assembly Test Chip Version 01 Description and User's Manual*, Sandia National Laboratories Report SAND90-0755, 1990.

[5] D. B. Fritz and C. S. Wang, "Performance of stable brominated epoxies in encapsulants for microelectronic devices,"in *Polymeric Materials for Electronics Packaging and Interconnection*, Eds. J. H. Lupinski and R. S. Moore, ACS Symposium Series 407, Washington, 1989, pp. 405-413.

[6] M. Nakao, T. Nishioka, M. Shimizu, H. Tabata, and K. Ito, "Degradation of brominated epoxy resin and effects on integrated-circuit-device wirebonds,"in *Polymeric Materials for Electronics Packaging and Interconnection*, Eds. J. H. Lupinski and R. S. Moore, ACS Symposium Series 407, Washington, 1989, pp. 421-428.


## DISCLAIMER

DATE
FILMED
6/22/94
END